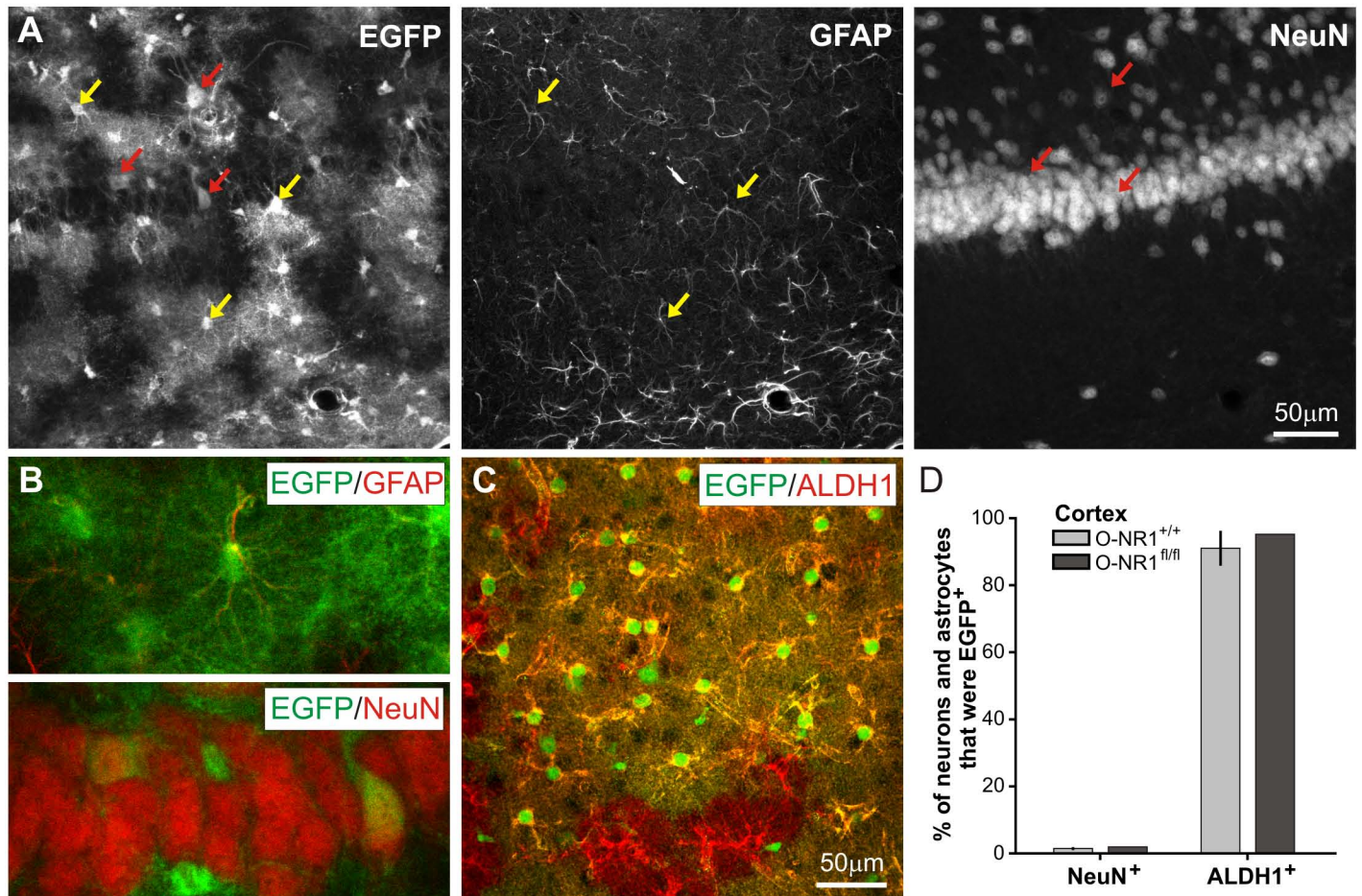
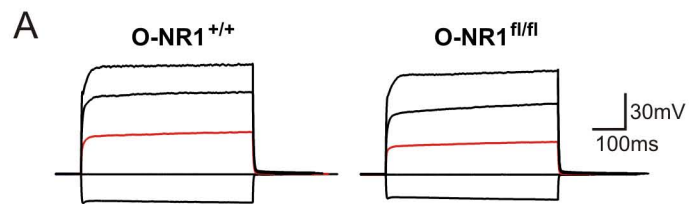


Supplementary Figure 1



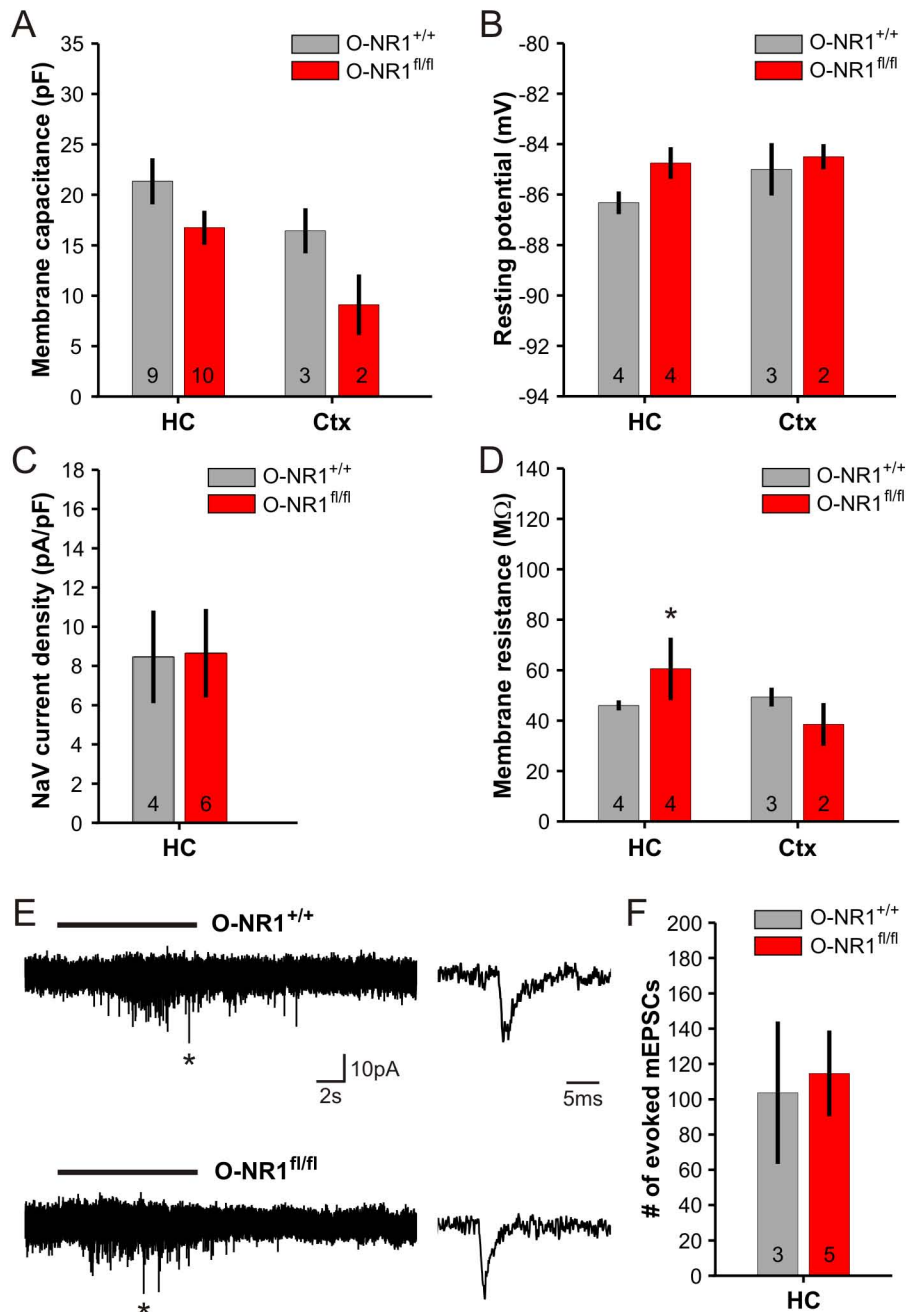
Supplementary Figure 1. Analysis of Cre-mediated recombination in *Olig1*^{cre/+} mice. *A*, EGFP expression within GFAP⁺ astrocytes and NeuN⁺ neurons in the hippocampus of O-NR1^{+/+} mice; yellow arrows highlight several GFAP⁺GFP⁺ cells and red arrows highlight several NeuN⁺GFP⁺ cells. *B*, Several GFAP⁺EGFP⁺ cells and NeuN⁺EGFP⁺ cells from *E* shown at higher magnification. *C*, EGFP expression within ALDH1⁺ astrocytes in the cortex of O-NR1^{+/+} mice. *D*, Graph showing the percentage of NeuN⁺ neurons and ALDH1⁺ astrocytes that express EGFP in the cortex of O-NR1^{+/+} and O-NR1^{fl/fl} mice.

Supplementary Figure 2



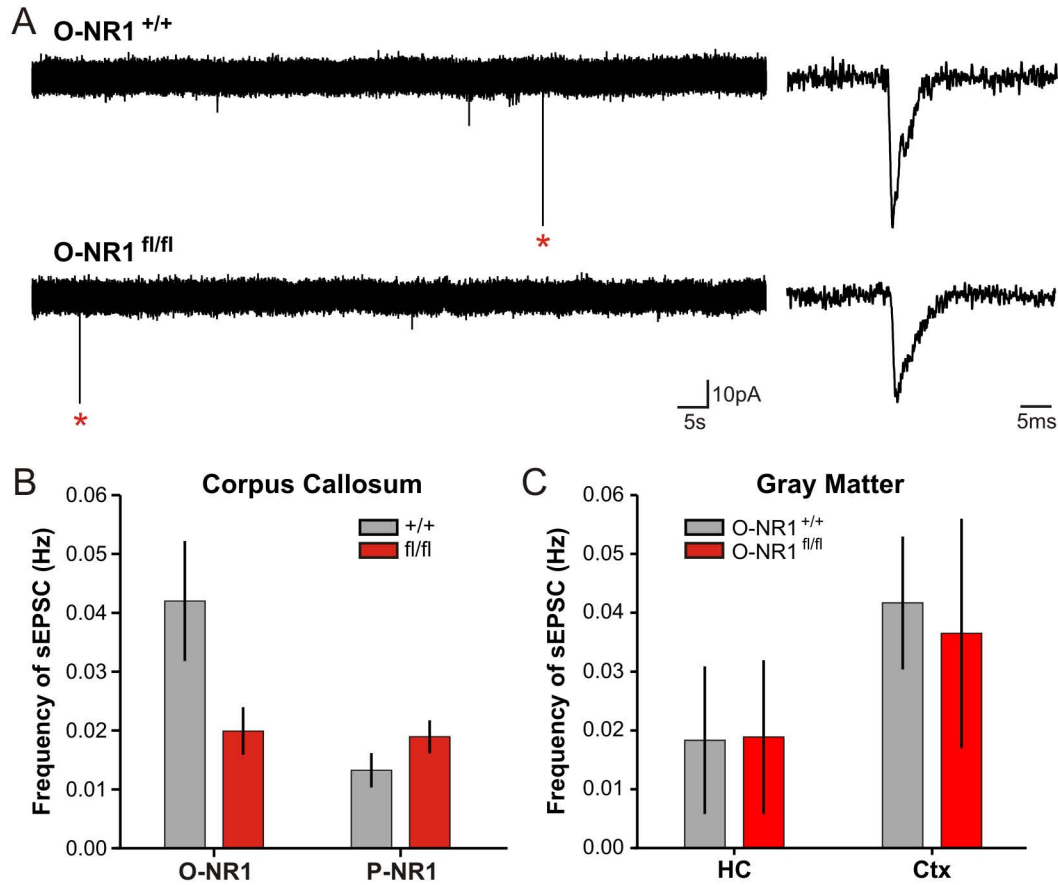
Supplementary Figure 2. Basic membrane properties of NMDAR-deficient OPCs following embryonic NMDAR ablation. Response of representative callosal OPCs in O-NR1^{+/+} and O-NR1^{fl/fl} mice to depolarization. Red trace = injection of 640pA.

Supplementary Figure 3



Supplementary Figure 3. NMDAR-deficient OPCs in gray matter display normal membrane properties and synaptic connectivity. *A-B*, Membrane capacitance (C_m) and resting membrane potential (V_m) of OPCs in CA1 hippocampus (HC) and cortex (Ctx) of mature (P40-45) O-NR1^{+/+} and O-NR1^{fl/fl} mice. Differences between genotypes were not significant (C_m HC, $p = 0.09$; C_m Ctx, $p = 0.15$; V_m HC, $p = 0.10$; V_m Ctx, $p = 1$). n indicated at the base of each column. *C*, Density of voltage gated sodium channels in hippocampal OPCs from mature O-NR1^{+/+} and O-NR1^{fl/fl} mice ($p = 0.92$). *D*, Membrane resistance of OPCs in HC and Ctx of mature O-NR1^{+/+} and O-NR1^{fl/fl} mice (Ctx, $p = 0.37$; HC, * $p = 0.03$). *E*, Response of hippocampal OPCs from O-NR1^{+/+} and O-NR1^{fl/fl} mice to application of hypertonic solution (HS, indicated by black bar). Asterisk indicates HS-evoked mEPSC shown at expanded time scale to the right. *F*, Quantification of the number of HS-evoked mEPSCs in hippocampal OPCs from O-NR1^{+/+} and O-NR1^{fl/fl} mice ($p = 1$).

Supplementary Figure 4.



Supplementary Figure 4. Spontaneous EPSCs persist in NMDAR-deficient OPCs. *A*, Two minute long recordings from representative callosal OPCs in mature (P40-45) O-NR1^{+/+} and O-NR1^{fl/fl} mice. Spontaneous excitatory post synaptic current (sEPSC) highlighted with red asterisk shown at expanded time scale to the right. *B*, Quantification of sEPSC frequency in callosal OPCs from control (O-NR1^{+/+}, P-NR1^{+/+}), constitutive (O-NR1^{fl/fl}), and inducible (P-NR1^{fl/fl}) NMDAR ablation mice. Differences between genotypes were not significant ($p = 0.054$, K-W ANOVA). *C*, Quantification of sEPSC frequency in OPCs from hippocampus (HC) and cortex (Ctx) of O-NR1^{+/+} and O-NR1^{fl/fl} mice. Differences between genotypes were not significant (HC $p = 1$, Ctx $p = 0.77$).